PRESSURE DISTRIBUTION AND HEAT EXCHANGE IN A GASDYNAMIC MODEL WITH COMBUSTION OVER WHICH A HIGH-ENTHALPY AIR STREAM FLOWS

V. K. Baev, V. V. Shumskii,
and M. I. Yaroslavtsev

UDC 536.46:621.45.022

In [1-3], on gasdynamic models with combustion in high-enthalpy oncoming air, we obtained the force characteristics, determined the completeness of hydrogen burning made a comparison of experimental and calculated data, and developed a physical picture of the flow in the internal channels of the models. The purpose of [1-3] was an investigation primarily of the total effect from hydrogen burning: thrust, migration of the pseudoshock on the initial section of the combustion chamber, and cutoff of the flow of air into the model.

In this paper we present data on the pressure distribution and heat fluxes in the channel of a gasdynamic model with combustion. The geometry of the internal channel is described in [1, 2]. But since the tests were conducted with the establishment of a short-lived regime and all the pressure sensors were located inside the model in order to reduce to a minimum the errors connected with the inertia of the pneumatic circuit, no free volume was left in the the model where a store of hydrogen could be placed, as in [1, 2]. Therefore, the model (Fig. 1) was built in the form of half an axisymmetric model of [1, 2] and placed on a lateral polypylon, through which hydrogen was supplied from an outside volume and the measurement cables were passed. The geometrical ratios of the internal channel of the model are $F_2/F_0 = 0.19$ and $\bar{F}_k = F_5/F_2 = 2.2$, where $F_0 = (1/2)(\pi d_0^2/4)$ is the area of the entrance to the model and F_2 and F_5 are the cross-sectional areas of the channel in cross sections 2 and 5, respectively. Methodological aspects of the measurement of the pressures, heat fluxes, and flow rates of the media through the model with an estimate of the errors occurring are presented in [4].

The tests were conducted in the same IT-301 pulsed tunnel [5] with a conical nozzle as the tests of [1, 2] and in the following range of the parameters of the oncoming air: stagnation pressure and temperature $P_{0o}(\tau) = 50\text{-}7$ MPa, $T_{0o}(\tau) = 1600\text{-}970$°K, Mach number $M_o = 7.9$, air flow rate through the model $m_a = 0.4\text{-}0.08$ kg/sec. Here τ is the current time of the regime (the reckoning was started from the instant of discharge of the condenser battery in the tunnel forechamber). The rate of decrease of p_{0o} and T_{0o} during the regime (just as in the tests of [1, 2]) is typical for pulsed tunnels and corresponds to the outflow of air with initial parameters $p_{0o}(0) = 50$ MPa and $T_{0o}(0) = 1600$°K from a forechamber with a volume of 1.14 dm^3 through a critical section 10 mm in diameter [5]. In Figs. 1-3 the hatched region a denotes the location of the hydrogen injectors in the model.

In Fig. 2 we present data on the distribution of the relative static pressure $\bar{p}_i = p_i/p_o$ (p_i is the pressure at the i-th cross section of the model and p_o is the static pressure of the oncoming air) over the central body of the model: 5-7) without a supply of hydrogen to the model; 1-4) in tests with hydrogen burning in the model with an excess-air coefficient $\alpha = 0.9$. Curve 7 is constructed from the results of a numerical calculation by the difference method of the flow of an ideal gas with an adiabatic $\varkappa = 1.4$.

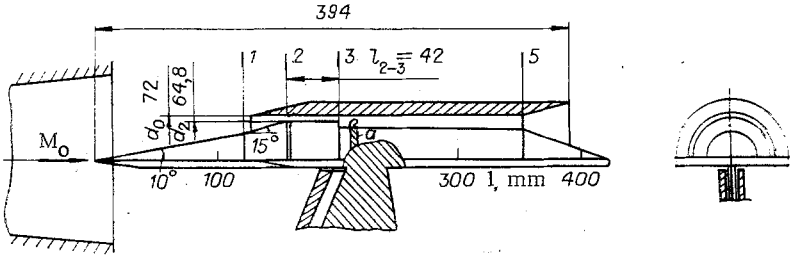

Fig. 1

Novosibirsk. Translated from Zhurnal Prikladnoi Mekhaniki i Tekhnicheskoi Fiziki, No. 5, pp. 56-65, September-October, 1985. Original article submitted July 3, 1984.

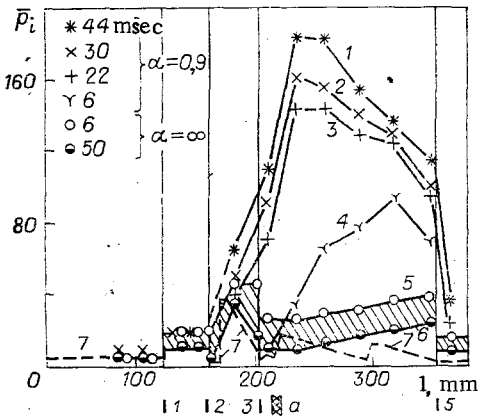

Fig. 2

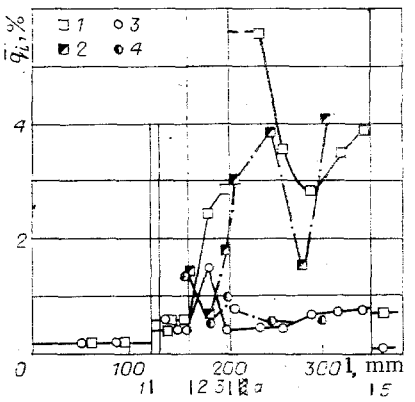

Fig. 3

The heat-flux distribution is shown in Fig. 3: 1, 3) in the central body; 2, 4) in the cowling of the internal channel of the model; 1, 2) in tests with combustion (α = 0.9-0.53, τ = 35-40 msec); 3, 4) in tests without combustion ($\alpha = \infty$); $\bar{q}_i = q_i F_0 / m_a h_{0_0}$ is the specific heat flux, where h_{0_0} is the specific stagnation enthalpy of the oncoming air. Physically, the quantity $\bar{q}_i$ represents the specific heat flux q_i at the corresponding point of the internal channel normalized to the stagnation enthalpy $m_a h_{0_0}/F_0$ carried by the oncoming air stream per second per square meter of cross section; or, $\bar{q}_i$ is the heat that escaped at the corresponding point of the internal channel through a surface with an area F_0 normalized to the stagnation enthalpy $m_a h_{0_0}$ entering the model with the oncoming stream.

An analysis of the experimental data on the pressure and heat fluxes in the internal channel in tests without a supply of hydrogen to the model yields the following.

1. The values of $\bar{q}_i$ at each point of the internal channel were constant during the entire regime (except for the surface of the second cone of the air intake at the time of migration of the boundary-layer separation from the throat to the compression surface; see below). Since the quantity $m_a h_{0_0}$ decreased in proportion to $p_{0_0}(\tau)\sqrt{T_{0_0}(\tau)}$ during the regime, the specific heat flux

$$q_i = \frac{\bar{q}_i}{F_0} m_a h_{0_0} = \alpha_{i,\alpha=\infty}(T_{0i}(\tau) - T_w) = \text{const}\, m_a h_{0_0}$$

at each point of the internal channel of the model is also proportional to $p_{0_0}(\tau)\sqrt{T_{0_0}(\tau)}$. Here $\alpha_{i,\alpha=\infty}$ is the heat-transfer coefficient in the i-th cross section; T_w is the wall temperature; $T_{0i}(\tau)$ is the air stagnation temperature in the i-th cross section; $T_{0i}(\tau) < T_{0_0}(\tau)$, since the air has cooled by heat transfer to the wall along the length of the model from the nose to the i-th cross section.

2. The measured pressure at the first and second cones of the air intake coincides with the calculated pressure. Here $\bar{p}$ remained constant at the first cone during the entire regime, while at the second cone it remained constant and equal to the calculated pressure only up to the value $\mathrm{Re} = v_0 l/\nu_0 \approx 2\cdot 10^6$ (up to 40-47 msec), where l = 0.165 m is the distance from the nose to cross section 2 along the generating lines of the first and second cones, and v_0 and ν_0 are the velocity and kinematic viscosity of the oncoming stream. Starting with $\mathrm{Re} \approx 2\cdot 10^6$, $\bar{p}$ at the second cone increased abruptly, from the value given by curve 7 for the second cone in Fig. 2 to the upper boundary of the hatched section. The abrupt change in the pressure at the second cone is connected with the abrupt shift in the separation of the boundary layer from the region of the throat of the air intake on the surface of the second cone. This shift of the separation was recorded by all pressure sensors located downstream. Starting from the time of the shift of the separation, the heat-flux sensors located on the second cone recorded an increase in $\bar{q}$, after which the new value of $\bar{q}$ remained constant up to the end of the regime.

3. In the initial section of the combustion chamber (between cross sections 2 and 3) there is a complex system of alternating shock waves and fans of rarefaction waves. The measured values of the pressure on the central body are in qualitative agreement with the calculated values. The peaks of the heat fluxes in this section correlated well with the pressure peaks.

4. The difference between the experimental and calculated pressures right in the combustion chamber (section 3-5) is connected with the fact that in the calculations we did not take into account viscosity, the separations of the boundary layer, and the injectors, which projected into the stream and were a strong retarding factor. The presence of friction, the separations, and the injectors leads to equalization of the pressure along the length of the chamber and smoothing of the sawtoothed pressure distribution obtained from calculations of an ideal gas. The distribution of $\bar{q}$ on section 2-5 is also smooth, without the peaks and valleys occurring in the initial section of the combustion chamber.

A property of the pressure distribution along the length of section 3-5 is a continuous increase in $\bar{p}$ during the regime, which is connected with the decrease in Re (from $\mathrm{Re} = 4.5 \cdot 10^6$ at $\tau = 0$ to $\mathrm{Re} = 1.5 \cdot 10^6$ at $\tau = 55$ msec) and the increase in $\bar{T}_w = T_w/T_{0i}$. These factors cause an increase in the air friction against the wall, resulting in an increase in the retardation of the supersonic stream in the chamber, and hence of p, during the regime.

An analysis of the experimental data on the pressure distribution for $\alpha = 1.3\text{-}0.22$ and on the heat fluxes for $\alpha = 1.3\text{-}0.53$ in the internal channel in the tests with hydrogen burning yields the following.

1. The measured pressure at the first cone of the air intake is higher ($\bar{p} = 6\text{-}9$) than the pressure at the first cone without a supply of hydrogen to the model ($\bar{p} = 4$). This is explained by the fact that during hydrogen burning the increased pressure from the chamber is transmitted to the compression surfaces through the subsonic zones existing in the corner configuration at the places where the conic surface joins with the lower plane of the model (see Fig. 1); these disturbances are transmitted to the drainage points through the boundary layer.

2. The measured pressures at the second cone are higher than $\bar{p}$ at the second cone for $\alpha = \infty$. This is connected, first, with the transmission of disturbances from the combustion chamber through the subsonic zones, as for the first cone, and second, with the migration of the separation from the throat of the air intake. Whereas for $\alpha = \infty$ the migration of the separation is connected with a decrease in Re, in the case of hydrogen burning in the model it occurs at $\tau \approx 10\text{-}15$ msec and is explained by "expulsion" of the separation to the compression surfaces by a pseudoshock moving on the initial section of the chamber: A stepwise increase in $\bar{p}$ at the second cone took place after the pressure sensors in section 2-3 recorded the movement of the start of the pseudoshock toward cross section 2. For $\alpha = 1.3\text{-}0.22$ the pressure $\bar{p}$ at the second cone after the shift of the separation due to the pseudoshock is about the same as the $\bar{p}$ that occurs for $\alpha = \infty$ after the shift of the separation due to the decrease in Re below $\sim 2 \cdot 10^6$ (see Fig. 2).

3. Despite the increase in $\bar{p}$ at the first cone for $\alpha = 1.3\text{-}0.22$ in comparison with $\bar{p}$ for $\alpha = \infty$, the values of $\bar{q}$ at the first cone are the same for $\alpha = \infty$ and 1.3-0.53 and equal ~ 0.002. Consequently, the operation of the combustion chamber does not affect the heat transfer to the first cone, although it does affect the pressure distribution over the first cone.

4. The values of $\bar{q}$ at the second cone for $\alpha = 1.3\text{-}0.5$ and $\tau > 10\text{-}15$ msec do not differ significantly from those values of $\bar{q}$ which would occur for $\alpha = \infty$ after the shift of the separation due to the decrease in Re.

5. In the initial section of the combustion chamber, especially for $\alpha < 1$, a considerable pressure rise is observed, occurring during the reorganization of flow in the combustion chamber from supersonic to subsonic. The quantity p_3/p_2 (p_3 is the pressure in cross section 3 and p_2 is that in cross section 2) comprises most of the pressure increase in the combustion chamber. It is also seen from Fig. 2 that the pressure in section 2-3 also grows continuously during the subsonic regime in the combustion chamber. This is connected with the movement of the pseudoshock toward cross section 2 due to the continuous increase in the heating of the working body [1, 2]. And the pressure sensors located in the region of cross section 3 recorded a process nonsteady in pressure, although the sensors located upstream and downstream did not record this, as a rule.

6. The heat-flux sensors located in the i-th cross section in section 2-3 reacted to the movement of the pseudoshock simultaneously with the pressure sensors located in the same cross section. Up to the arrival of the pseudoshock at this cross section, the value of $\bar{q}_i$ is close to the value of $\bar{q}_i$ at this point for $\alpha = \infty$. But after the pseudoshock arrived at this cross section, the values of $\bar{q}_i$ grew rapidly (see Fig. 3). Thus, in the region of cross section 3, $\bar{q}_i$ at the central body for $\alpha \leqslant 1$ increased by a factor of 4-10 (as a function of τ)

compared with tests for $\alpha = \infty$. A considerably smaller increase in $\bar{q}_i$ occurred at the cowling, indicating the considerably nonuniform retardation of the supersonic stream in the initial section of the combustion chamber: The retardation of the air stream in layers located near the central body begins closer to cross section 2 than in layers located near the cowling.

7. Right in the combustion chamber in section 3-5 a further pressure rise was observed from cross section 3 to a point located 30-50 mm below cross section 3. After this point the pressure falls, and at the exit from the chamber (in cross section 5) it reaches 0.6-0.7 of the maximum pressure in section 3-5.

The maximum value of $\bar{p}_i$ in section 3-5 (and hence in the entire internal channel of the model) for the range of α = 1.3-0.22 occurred for α = 0.4-0.6 and comprised $\bar{p}$ = 190. For α = 1 the maximum value was $\bar{p}$ = 175, i.e., ∿8% lower. Calculated estimates of the pressure in characteristic cross sections of the combustion chamber made by the method of [6] showed that for the same completeness of combustion ξ the pressure increase in the characteristic cross sections of the chamber in the transition from α = 1 to α = 0.5 is ∿5%, i.e., in these tests the increase in the amount of hydrogen burned for $\alpha < 1$ in comparison with the amount of hydrogen burned for α = 1 was insignificant. This is also indicated by the heat-flux measurements: In the range of α = 1-0.53 the relative heat lost to the wall of section 3-5 comprised the same amount.

This character of the pressure distribution along the length of section 3-5 due to a number of factors. First, from data obtained on attached manifolds [7, 8] it follows that a considerable share of the heat was released over a length comparable to the length of the pseudoshock. Second, there was considerable removal of heat to the chamber walls. Both these factors lead to strong nonuniformity of the heat supply to the working body along the length of the chamber. Third, the frictional force and local hydraulic resistances acted on the moving gas. Fourth, supply of heat to the subsonic stream results, just like friction, in acceleration of the gas with a corresponding pressure drop. Fifth, in cross section 3 the pseudoshock has not yet ended, but extended below cross section 3 with the corresponding pressure drop along its length. The combination of these factors led to the complicated variation of $\bar{p}$ along the length of the combustion chamber.

8. Whereas for $\alpha = \infty$ the quantities $\bar{q}_i(\tau)$ were constant during the regime, for α = 1.3-0.53 they increased with an increase in τ at all points of the combustion chamber. In fact,

$$\bar{q}_i \approx \frac{\alpha_{i,\alpha}(T_{0i}(\tau) - T_w)}{p_{0_0}(\tau)\sqrt{T_{0_0}(\tau)}} \approx \left(\frac{\alpha_{i,\alpha}(T_{0i}(\tau)_{\alpha=\infty} - T_w)}{p_{0_0}(\tau)\sqrt{T_{0_0}(\tau)}} + \frac{\alpha_{i,\alpha}\xi_i H_u}{\alpha^{\nu} L_0 \frac{\alpha+1}{\alpha} c_p p_{0_0}(\tau)\sqrt{T_{0_0}(\tau)}}\right), \quad (1)$$

where $\alpha_{i,\alpha}$ is the heat-transfer coefficient for α = 1.3-0.53; $\xi_i H_u$ is the heat released in the combustion chamber up to cross section i; ξ_i is the completeness of combustion reached by cross section i; U_u is the calorific effect of the reaction; L_0 and c_p are the stoichiometric coefficient and the specific heat; ν = 1 for $\alpha \geqslant 1$; ν = 0 for $\alpha < 1$. In hydrogen burning $T_w \approx T_{w,\alpha=\infty}$, since the walls were unable to heat up significantly in a time of 50 msec; $\alpha_{i,\alpha} > \alpha_{i,\alpha=\infty}$, since for a turbulent boundary layer $\alpha_i \sim p_i^{0.8}$, while p_i is the combustion chamber for α = 1.3-0.53 is larger than p_i for $\alpha = \infty$ by a factor of 3-15. Therefore, from (1) we have

$$\bar{q}_i \approx \frac{\alpha_{i,\alpha}}{\alpha_{i,\alpha=\infty}} \bar{q}_{i,\alpha=\infty} + \Delta\bar{q}_i > \bar{q}_{i,\alpha=\infty}.$$

Moreover, it follows from Eq. (1) that for those points of the combustion chamber for which the value of $\alpha_{i,\alpha}$ is higher than at neighboring points, not only will the value of $\bar{q}_i$ be higher than at neighboring points, but also its rate of increase during the regime. For the tests made with α = 1.3-0.53 the highest values of $\bar{q}_i$ and of its rate of growth during the regime were observed in the part of the central body (the "hottest" point) which was 30-50 mm away from cross section 3 and coincided with the point of maximum pressure in the chamber, while the lowers $\bar{q}_i$ (the "coolest" point in the chamber) was observed in sections of the cowling located in the middle of the combustion chamber. In comparison with tests for $\alpha = \infty$, the values of $\bar{q}_i$ with hydrogen burning with $\alpha \leqslant 1$ were increased at τ = 35-40 msec by a factor of ∿12 for the "hottest" spot and by ∿2.3 for the "coolest."

It is seen from Fig. 3 that toward the end of the combustion chamber the heat flux has increased again, since the pylons which supported the cowling were located at this point in the chamber. Since the stream is subsonic in the chamber, the pylons had practically no influence on the pressure distribution, but they significantly affected the distribution of $\bar{q}_i$.

TABLE 1

Sections of surface of the internal channel			$\frac{S_n}{F_*}$	$\overline{Q}_i$, %										
				α										
				∞	1,3		1,1		0,77		0,66		0,53	
				τ, msec										
n	designation			0—50	15	40	15	40	15	40	15	40	15	35
1	Air intake		5,56	1,63	1,45	1,97	1,45	1,97	1,13	2,53	1,45	2,53	1,45	1,97
2	Section 2-3	Central body	2,09	1,98	4,08	5,3	4,2	4,4	3,34	4,2	4,2	6,7	3,76	5,64
		Cowling	2,33	2,16	2,33	2,8	3,3	3,7	3,26	3,5	2	2,8	2,33	2,33
3	Section 3-5	Central body	6,16	3,88	15,4	19,1	16,1	24,6	19,8	22,1	18,5	26,5	17,6	22,5
		Cowling	8,11	4,06	13	16,2	18,6	23,5	18,6	23,7	18,6	26,8	21,9	27,3
4	Nozzle		4,53	0,45	3,4	3,4	2,7	2,7	3,3	3,3	3,3	3,3	2,7	2,7
$\overline{Q}_1$, %				14,2	39,7	48,8	46,4	60,9	49,3	59,2	47,9	68,5	49,7	62,4
$\overline{Q}_2$, %				—	21,2	20,5	21	21,7	20,3	19,2	19,7	22,2	20,5	21
					Mean value ($20.7 + \sigma = 0.3$)									

In Table 1 we present data on the heat losses in each of the four sections of the internal channel of the model, giving separate data for the central body and for the cowling for the combustion chamber. The total heat losses in each section are $\bar{Q}_i = \sum_i q_i S_i/(m_a h_{0o})$, where S_i is the area of the lateral surface of the internal channel for which the values of q_i were taken as constant; the values of S_n/F_0 for each are given in a separate column. In the absence of a hydrogen supply, the $\bar{q}_i$ were constant during the entire regime, and the data in the $\alpha = \infty$ column are valid for the entire regime of operation of the model. With hydrogen burning in the model the $\bar{q}_i$ varied during the regime. Therefore, two q_i are given for each α: at $\tau = 15$ msec, when the transition from supersonic to subsonic flow is nearly completed [1, 2], and at $\tau = 40$ msec (at $\tau = 35$ msec for tests with $\alpha = 0.53$, since the cutoff of air flow into the model took place at $\tau = 34$-36 msec for this α), when the flow in the combustion chamber was subsonic.

As is seen from Table 1, for $\alpha = \infty$ the total relative heat flux $\bar{Q}_1$ through the walls of the internal channel of the model is relatively small (14.2%),

$$\bar{Q}_1 = \frac{\sum_n \sum_i q_i S_i}{m_a h_{0o}},$$

but during hydrogen burning it increased considerably, and for $\alpha \leqslant 1$ it comprised 50-60% at $\tau = 15$-40 msec.

An interesting fact is the independence from α and τ of the quantity $\bar{Q}_2$, the heat flux to the walls of the model normalized to the heat which could be released by hydrogen burning with $\xi = 1$:

$$\bar{Q}_2 = \frac{\sum_n \sum_i q_i S_i}{m_a H_u/\alpha^{\nu} L_0}.$$

An analysis made for the ranges of $\alpha = 1.3$-0.53 and $\tau = 15$-40 msec, i.e., for practically all the available regimes of hydrogen burning in the model, showed that $\bar{Q}_2 = 0.207$ with an rms deviation of 0.003 (0.003/0.207 = 1.4%). The fact of the independence of $\bar{Q}_2$ from α and τ is evidence of the following:

1. The losses in the combustion chamber are determining in the heat fluxes to the walls of the internal channel of the model during hydrogen burning.

2. The completeness of combustion in the range of $\alpha = 1.3$-0.5 is about the same and constant during the time $\tau = 15$-40 msec under consideration, confirming the conclusion of $\xi = \text{const}$ for $\alpha = 1$-0.5 obtained from a comparison of the maximum values of $\bar{p}$ for $\alpha = 1$ with the maximum values of $\bar{p}$ for $\alpha = 0.4$-0.6.

In Fig. 4 the heat losses in different sections of the internal channel of the model are represented graphically: 1) at the surface of the air intake; 2) at the wall of the initial section of the combustion chamber; 3) at the wall of section 3-5 of the combustion chamber; 4) at the surface of the nozzle:

$$\bar{Q}_{1n} = \frac{\sum_i q_i S_i}{m_a h_{0c}}, \quad \bar{Q}_{2n} = \frac{\sum_i q_i S_i}{m_a H_u/\alpha^{\nu} L_0}, \quad n = 1 - 4.$$

It is seen from Fig. 4, as well as from Table 1, that the main heat losses to the walls of the internal channel of the model took place right in the combustion chamber.

The results of the present measurements of the heat fluxes to the surfaces of the air intake can be compared with the data of [9], where the heat fluxes to the surfaces of air intakes with $F_2/F_0 = 0.066$ and 0.078 were measured for $M_0 = 7$. In [9] it was shown that for Re comparable with the Re in the present tests, heat comprising 0.6-0.8% of the enthalpy of the air entering the model was lost to the walls of the air intake (up to cross section 2). In the present tests this quantity was $\sim$1.6%, in qualitative agreement with the data of [9], since it was shown there that separation zones, blunting, and turbulizers can increase the amount of heat lost in the air intake by a factor of two to five.

The parameters of the air in the combustion chamber were determined, with the distributions of pressure and heat fluxes along the length of the model known from the tests, from the equations of conservation of mass, energy, and change in momentum, written for a control

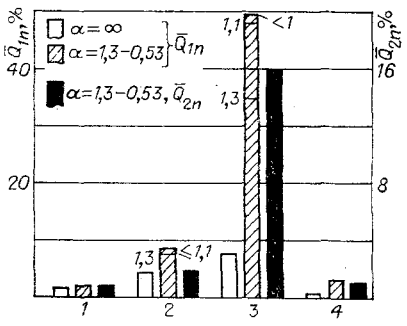

Fig. 4

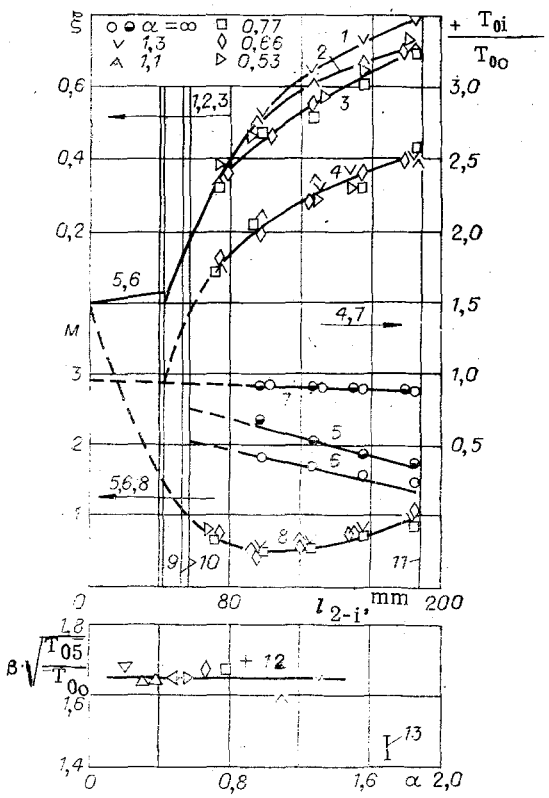

Fig. 5

volume bounded by the chamber walls, cross section 2, and the current cross section i. For $\alpha = \infty$ the system has the form

$$m_a = m_i, \quad m_a v_i - m_2 v_2 = p_2 F_2 - p_i F_i + \int_2^i p dF - X_{fl},$$

$$m_a h_{0i} = m_a h_{0o} - Q_w,$$

where $X_{f\ell}$ is the frictional resistance and the local resistance in the chamber over the length from cross section 2 to cross section i; Q_w are the heat losses to the walls of the internal channel up to the i-th cross section; v is the velocity. This is the sequence of the calculations: From the energy equation with the Q_w known from the tests we determined T_{0i}, then from the equation of conservation of mass we determined M_i, and from the equation of change in momentum we determined $X_{f\ell}$.

The results of the calculation of T_{0i} and M_i for $\alpha = \infty$ along the length of the chamber are presented in Fig. 5: 5, 6) M_i; 7) T_{0i}/T_{0o}; 9-11) locations of cross section 2, the injectors, and cross section 5, respectively.

In section 2-3 the air is accelerated from $M_2 = 3.98$ to $M_3 = 4.18$ (the values of M in section 2-3 were obtained from a numerical calculation of the flow and averaging over its cross section). Then the stream is expanded additionally in flow over a step. However, the system of injectors projecting into the stream results in considerable retardation of the supersonic flow in shock waves. The strong shock waves traveling from the injectors into the stream are well seen in the soot–oil coatings deposited in the series of tests. Therefore, in the region of the injectors curves 5 and 6 are given with a break. Since the pressure in the chamber increases during a regime, the Mach numbers in the chamber fall with an increase in τ: Curves 5 and 6 correspond to $\tau = 40$ and 50 msec.

From curve 7 it is seen that at the exit from the combustion chamber the stagnation temperature of the air is ∿13% lower than the temperature T_{0o} owing to heat transfer from the air to the cool walls of the model. And this decrease in air temperature takes place mainly in the the combustion chamber, since at the compression surfaces (up to cross section 2) the stagnation temperature decreases by only ∿1.6% (also see Table 1).

For hydrogen burning in the model the system of equations for determining the parameters along the channel of the combustion chamber has the form

$$m_a + m_{H_2} = m_i, \quad m_i v_i - m_a v_2 - m_{H_2} v_{H_2} = p_2 F_2 + p_{H_2} F_{H_2} - p_i F_i + \int_2^i p dF - X_{fl},$$
$$m_i h_{0i} = m_a h_{0o} + m_{H_2} h_{H_2} - Q_w + \frac{m_a}{\alpha^{\nu} L_0} H_u \xi_i, \tag{2}$$

where the index H_2 refers to hydrogen. This is the sequence of the determination of the stream parameters from the system (2). At the exit from the combustion chamber $M_5 = 1$. On this basis and taking the exit from the combustion chamber as the i-th cross section, from the second equation of the system (2) we determine $X_{f\ell}$ for the entire chamber. It is assumed that $X_{f\ell} \sim S_{2-i}$, where S_{2-i} is the area of the lateral surface of the combustion chamber from cross section 2 to cross section i. This is justified by the fact that $Y_{f\ell}$ for tests with burning is lower than for tests with $\alpha = \infty$ by a factor of five to six. For $\alpha = \infty$ the wave resistance of the injectors and pylons over which the supersonic stream flows makes up the main share in $X_{f\ell}$. In the tests with combustion, a subsonic stream flows over the pylons and injectors, so wave resistance is absent: Friction makes the main contribution to $X_{f\ell}$. Then M_i are determined from the second equation, T_{0i} from the first, and ξ_i from the energy equation.

The results of the determination of ξ_i, T_{0i}/T_{0o}, and M_i are presented in Fig. 5: 1-3) ξ_i; 4) T_{0i}/T_{0o}; 8) M_i; for $\alpha < 1$ the data were taken at $\tau = 35$-40 msec, while for $\alpha > 1$ they were taken at $\tau = 50$ msec.

In [1, 2] it was shown, as a result of direct photography of the flame through a window in the model, that for $\alpha = 1.7$-3 the flame did not back up to the initial section of the chamber. Therefore, the curves of burnup (1-3) and relative temperature (4) are brought up to cross section 3, above which there are no burning. For $\alpha < 1$ the values of ξ_i for different α fit onto one curve. This, and the fact that the burnup curves are not significantly layered for $\alpha > 1$, confirm the conclusion, obtained from an analysis of the distributions of pressure and heat fluxes, that the completeness of combustion is the same in the range of $\alpha = 1.3$-0.5. The values of $\xi = 0.7$-0.8 determined in the present tests for $\alpha = 1.3$-0.53 coincide with the data of [1, 2], obtained under close conditions by the weight method.

During hydrogen burning in the model the supersonic stream in the initial section of the chamber is retarded in the pseudoshock from the value of $M_2 = 3.98$ to the minimum value $M_{min} \approx 0.6$, lying at a distance of 30-50 mm below cross section 3. With allowance for the fact that the injectors and the step result in considerable nonuniformities of the stream in the cross sections, the dependence of M on ℓ_{2-i} in the section of M_2-M_{min} is drawn with a dashed line, which only reflects the general tendency for M to decrease along the length of the chamber from M_2 to M_{min}.

The cutoff of air flow into the model was observed in all the tests with burning and took place at different τ and T_{0o} for different α. However, the complex $\beta\sqrt{T_{05}/T_{0o}}$, where $\beta = (m_a + m_{H_2})/m_a$, at the time of cutoff of inflow remained constant for all the tests (curve 12). In Fig. 5 we present data from [1, 2] (line 13) on the cutoff of flow into a model having a combustion chamber with a lower expansion ratio $\overline{F}_c = 1.88$, and these correlate with the results of the present work, since the smaller the $\overline{F}_c$, the lower the values of $\beta\sqrt{T_{05}/T_{0o}}$ at which the cutoff of flow into the model should occur.

For the present model with $\overline{F}_c = 2.2$ the limiting value of the complex $\beta\sqrt{T_{05}/T_{0o}}$ at which thermal blocking of the chamber with a level of losses $X_{f\ell}/p_0F_0 \approx 5$ is still absent equals 2.53. The fact that immediately before the cutoff of air flow into the model the value of $\beta\sqrt{T_{05}/T_{0o}} = 1.65$ is considerably less than the limiting possible value is a confirmation of the fact, discovered in [1, 2], that the cutoff of inflow did not occur due to thermal blocking of the combustion chamber. The cause of the cutoff was that the zone in which the transition of the flow from supersonic to subsonic took place, due to the heat supply to the combustion chamber, lay too close to cross section 2.

The authors thank I. K. Yaushev for help in calculating the flow in the model for $\alpha = \infty$.

LITERATURE CITED

1. V. K. Baev, V. V. Shumskii, and M. I. Yaroslavtsev, "Gasdynamics of a model with combustion in a pulsed wind tunnel," Zh. Prikl. Mekh. Tekh. Fiz., No. 6 (1983).
2. V. K. Baev, V. V. Shumskii, and M. I. Yaroslavtsev, "Operation of a two-regime combustion chamber in the subsonic regime of heat supply," in: Gasdynamic Flows in Nozzles and Diffusers [in Russian], Inst. Teor. Prikl. Mekh., Sib. Otd. Akad. Nauk SSSR, Novosibirsk (1982).

3. V. K. Baev, V. V. Shumskii, and M. I. Yaroslavtsev, "Force characteristics and flow parameters in the channel of a model with combustion," Zh. Prikl. Mekh. Tekh. Fiz., No. 1 (1984).
4. V. K. Baev, V. V. Shumskii, and M. I. Yaroslavtsev, "Methodological problems of the testing of aerodynamic models with combustion in high enthalpy installations in a short-time regime," Izv. Sib. Otd. Akad. Nauk SSSR, Ser. Tekh. Nauk, Issue 1, No. 4 (1984).
5. A. S. Korolev, B. V. Boshenyatov, I. G. Druker, and V. V. Zatoloka, Pulsed Tunnels in Aerodynamic Research [in Russian], Nauka, Novosibirsk (1978).
6. Yu. A. Saren and V. V. Shumskii, "Characteristics of a GPVRD with a two-regime combustion chamber," Gasdynamic Flows in Nozzles and Diffuses [in Russian], Inst. Teor. Prikl. Mekh., Sib. Otd. Akad. Nauk SSSR, Novosibirsk (1982).
7. V. K. Baev, G. V. Klimchuk, et al., "Diffusional combustion in a plane channel with sudden expansion," Fiz. Goreniya Vzryva, 12, No. 3 (1976).
8. V. L. Zimont, V. M. Levin, and E. A. Meshcheryakov, "Hydrogen burning in supersonic stream in a channel in the presence of a pseudoshock," Fiz. Goreniya Vzryva, 14, No. 4 (1978).
9. V. G. Gurylev and N. N. Shkirin, "Heat fluxes in hypersonic air intakes with turbulizers and blunting of the central body," Uch. Zap. Tsentr. Aerogidrodin. Inst., 9, No. 4 (1978).

HEAT EXCHANGE AT THE LATERAL SURFACE OF A BLUNT CONE DURING ABSORPTION OF THE ENTROPY LAYER BY THE LAMINAR AND TURBULENT BOUNDARY LAYER

Yu. N. Ermak, N. P. Kolina, and A. Ya. Yushin

UDC 532.526-3.011.7

The entropy layer on a blunt body has a strong influence on flow in the boundary layer. In particular, allowance for absorption of the entropy layer leads to an increase in the heat flux [1-4]. The papers [1-3] are devoted to an investigation of this phenomenon in the laminar flow regime, while in [4] the influence of absorption of the entropy layer is analyzed for flow in the boundary layer with both a laminar and a turbulent character. This influence of absorption of the entropy layer on the heat flux is especially pronounced in a turbulent flow regime. It is advisable to make an experimental test of the calculated data of [1-4] by comparing the results of experiment and calculation for the same flow conditions. In the present paper such a comparison of experimental and calculated results, represented in similarity parameters, is made for the conditions of a shock tube at $M_\infty = 6.1$ and 8.

The shock tube operated on a pulsed scheme. The duration of the steady state of tube operation was $\sim$0.02 sec. The model consisted of a spherically blunted circular cone with an aperture half-angle $\theta = 10°$ and a blunting radius $r = 3$ and 5 mm. The length of the model was 285.7 and 276.2 mm for $r = 3$ and 5 mm, respectively. For $M_\infty = 6.1$ the stagnation temperature was 564 and 730°K, the total pressure was varied in the range from $1.6 \cdot 10^6$ to $14 \cdot 10^6$ Pa, while the Reynolds number R_∞, calculated from the parameters of the undisturbed stream and the blunting radius, varied from $2.1 \cdot 10^4$ to $3.1 \cdot 10^5$. In the case of $M_\infty = 8$ the stagnation temperature was $T_0 = 737$°K, the total pressure was $9.5 \cdot 10^6$ and $14.5 \cdot 10^6$ Pa in the tests with $r = 3$ and 5 mm, respectively, and $R_\infty \simeq 1 \cdot 10^5$. The temperature factor t_w, expressed as the ratio of the enthalpy h_w of the surface of the cone to the stagnation enthalpy H_0 of the oncoming stream, was 0.40 and 0.52 for $T_0 = 730$ and 564°K.

On the test model we mounted 40 calorimetric converters (sensors) arranged along one generating line. The calorimetric converters were built in the form of a copper disk 2 mm in diameter. A microthermocouple was welded to the inner side of the disk in a point weld. Both its thermoelectrodes (Chromel and Copel) were rolled to a thickness of 0.03 mm and a width of 0.2 mm at the point of the weld. To install the converters* on the model we drilled openings 2.6 mm in diameter in its wall. A disk was fastened into an opening with epoxy

*Converters of this type were developed by Yu. Yu. Kolochinskii, and the experiment in the tube was carried out with his participation.

Moscow. Translated from Zhurnal Prikladnoi Mekhaniki i Tekhnicheskoi Fiziki, No. 5, pp. 65-69, September-October, 1985. Original article submitted July 4, 1984.

